DYNAMICS OF ZIRCONIA NANOPARTICLES MADE BY FLAME SPRAY PYROLYSIS

Martin C. Heine, Roger Mueller, Rainer Jossen, Sotiris E. Pratsinis*

* Particle Technology Laboratory, ETH Zürich, CH-8092 Zürich, Switzerland

ABSTRACT

The growth of zirconia primary particles made in spray flames at relatively high production rates of (100 and 300 g/h) is studied by thermophoretic sampling (TS) and image analysis of transmission electron microscope (TEM) pictures. At each TS location, the corresponding temperature of the particle-laden spray flame is measured by Fourier transform infrared (FTIR) spectroscopy while the final product powder is analyzed by nitrogen adsorption and TEM. The evolution of primary and agglomerate ZrO_2 size distribution in spray flames is presented and explained quantitatively accounting for aerosol coagulation and sintering.

1. INTRODUCTION

Flame spray pyrolysis (FSP) is one of the promising techniques for synthesis of a broad spectrum of functional inorganic nanoparticles as it overcomes the need of gaseous precursors that is required by the industrially established flame reactors for synthesis of nanostructred commodities. Though some systematic studies on understanding the role of process parameters on the characteristics of product particles have been carried out [1] and even scale-up of FSP has been addressed [2], FSP has been treated so far as a "black" box. Essentially little is known on how droplets are converted to particles as *in-situ* measuring of flame and particle characteristics is rather challenging in these particle-laden flames. Such data are needed to understand some of the intriguing FSP results such as the formation of solid or hollow Al_2O_3 by replacing air with O_2 as oxidant/dispersion gas [3, 4] or Bi_2O_3 by controlling the composition of the precursor solution fed to FSP [5].

Synthesis of ZrO_2 particles is studied here [6] as ZrO_2 is a basis material in catalysts, oxygen sensors, fuel cells, resistive heating elements and even jewelry for its high oxygen ion conduction and high refractive index [7-10].

The objective of the present study is to investigate ZrO_2 particle growth inside spray flames at relatively high production rates by thermophoretic sampling (TS) and image analysis of transmission electron microscope (TEM) pictures [11]. These data are compared to a quantitative description of ZrO_2 primary and agglomerate particle growth accounting for aerosol coagulation and sintering [12] during FSP after evaluation of ZrO_2 sintering data from the literature.

2. EXPERIMENTAL

The spray apparatus consists of a commercially available external-mixing stainless steel gas assisted nozzle (Schlick-Düsen).The dispersion gas (O_2) flow rate is 25 and 50 l/min. The nozzle is surrounded by two stainless steel annuli forming a diffusion flame when 2 l/min of CH_4 flows through the inner and 4.5 l/min of O_2 flows through the outer annulus. Additional sheath O_2 (15 l/min) is fed through a sintered metal plate ring with inner-outer diameter of 28-50 mm surrounding the previous outer annulus. Zirconium n-propoxide ($Zr(C_3H_7O)_4$, 70 wt% in n-propanol) is used as precursor and is dissolved in ethanol (EtOH) resulting in precursor solutions of 0.5 M. The liquid precursor solution feed rate ranged from 27.1 to 81.1 ml/min resulting in ZrO_2 production rates from 100 to 300 g/h. A 1 liter precision piston pump (Isco, Inc., 1000D) is used for pulsation-free supply of the precursor solution. Product powders are collected in a commercial Jet filter (Friedli AG, FRR 4/1.2) consisting of four PTFE (polytetrafluoroethylene, Teflon) coated Nomex baghouse filters which are cleaned periodically by air pressure shocks.

3. THEORY

Assuming rapid droplet evaporation and zirconium n-propoxide oxidation, the product ZrO_2 particles grow by monomer- and cluster-cluster collisions neglecting the spread of the primary and agglomerate size distribution. Thus, the evolution of the average primary and agglomerate particle diameters can be described by coagulation and sintering as in gas-fed flame aerosol reactors [12]. Therefore, the particle number concentration, N (# particles/kg_{gas}), decreases by coagulation:

$$\frac{dN}{dt} = -\frac{1}{2}\beta N^2 \rho_{gas} \tag{1}$$

where ρ_{gas} (kg/m^3) is the gas density at temperature T and β (m^3/s) is the collision frequency function for Brownian coagulation given by the Fuchs interpolation function from the free-molecular to the continuum regime [13]. Likewise, the evolution of the total particle area concentration, A (m^2/kg_{gas}) is [12, 14]:

$$\frac{dA}{dt} = -\frac{1}{\tau_s}(A - N \cdot a_s) \tag{2}$$

where τ_s (s) is the characteristic sintering time for ZrO_2. The average volume v (m^3) of agglomerated particles is $v = V/N$. The primary particle diameter, d_p (m), the number of primary particles per agglomerate, n_p, and the agglomerate diameter, d_a, are [12]:

$$d_p = \frac{6v}{a},\ n_p = \frac{a^3}{36\pi v^2},\ d_a = d_p(n_p^{1/D_f}) \tag{3}$$

The axial gas velocity profile u (m/s) of the spray as a function of height above the nozzle (HAN), x, is obtained from a correlation for turbulent jets issuing from a round nozzle [15] corrected for the spray flame temperature [6].
Equations (1) and (2) are solved by VODPK software [16] with the initial conditions (x = 0 cm (100 and 300 g/h); x = 5 cm (100 g/h) and x = 7.5 cm (300 g/h)): $N = N_0 = ((S/1000)\cdot c\cdot N_A)/(F\cdot\rho_{gas}(0))$, $V = V_0$, $A = A_0$, where N_0 is the initial monomer (molecule) concentration of ZrO_2, and A_0 and V_0 are the equivalent-sphere surface area and volume, respectively, of all ZrO_2 molecules.

This model is attractive for its simplicity, computational efficiency and accuracy (within 10%) for predicting the particle diameter in gas phase processes especially at high temperatures [17].

4. RESULTS AND DISCUSSION

4.1. Spray flame characteristics and growth of FSP-made ZrO_2

Increasing the liquid (solution) feed rate from 27.1 to 81.1 ml/min (increasing the ZrO2 production rate from 100 to 300 g/h) increases the spray flame height from 13 to 37 cm. Detailed temperature profiles have been measured by FTIR for these conditions [6].

In contrast to gas-fed flame aerosol reactors, with spray flames thermophoretic sampling (TS) is only possible at locations where the droplets are completely evaporated e.g. at and above x = 7.5 and 10 cm for the production rate of 100 and 300 g/h, respectively, otherwise the carbon coated TEM grids are destroyed by the burning droplets depositing on them. Therefore, monitoring the evolution of particle growth in the early stages of the spray flame was not possible.

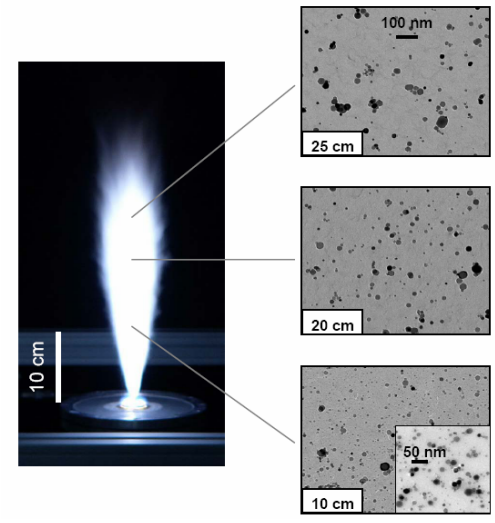

Fig. 1 ZrO_2 particles collected by thermophoretic sampling at x = 10, 20, 25 cm height above nozzle at a production rate of 300 g/h (adapted from [6]).

Figure 1 show TEM pictures from TS along the flame axis for a production rate of 300g/h. No hollow particles or shell fragments were observed throughout the process. The primary particle size increases with increasing x by gas phase or surface reaction, coagulation, and sintering as in gas-fed premixed flames [18]. In the luminous part of the spray flames, single spherical particles are observed, while further downstream agglomeration of primary particles can be seen, starting approximately at x = 15 cm for the 100 g/h flame and at about 40 cm (Fig. 1) for the 300 g/h flame. However, limited necking between those broadly-sized primary particles is observed indicating a low degree of agglomeration [6].

Particles made at 300 g/h are significantly larger than those made at 100 g/h at all locations and on the filter. Increasing the production rate by increasing the liquid feed rate results in a higher enthalpy content of the flame that leads to longer particle residence times at high temperatures [6] increasing the particle sintering rate results in the formation of larger particles. Furthermore, the precursor concentration increases and therefore the ZrO_2 concentration leading to faster coagulation and therefore enhanced particle growth that increases the particle diameter especially when complete coalescence takes place [19].

Figure 2 shows the evolution (TS/TEM counting (open symbols) and BET-measurements (filled symbols)) of the corresponding Sauter mean primary particle diameter, d_s as a function of x for a ZrO_2 production rate of 300 g/h (circles) along with the theoretical model prediction of d_s (solid lines). The standard deviation of multiple reproduction (error bar) is typically so small (< 3%) that it is smaller than the symbol in the figure.

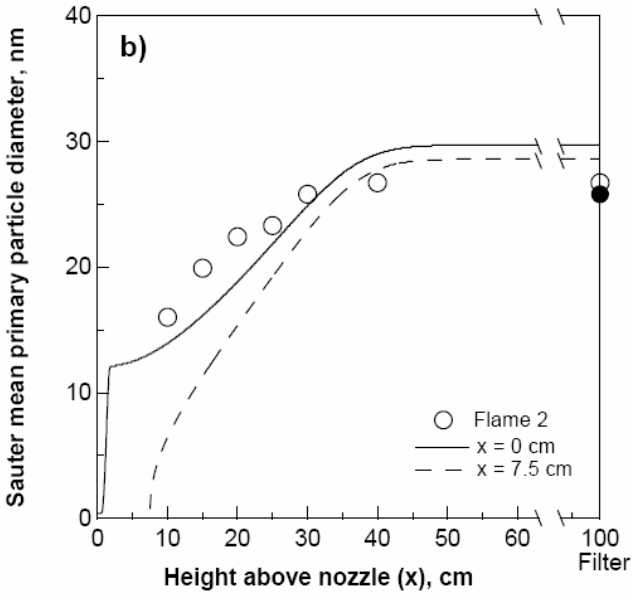

Fig. 2 Calculated evolution of the primary particle Sauter mean diameter, d_S, along the flame axis for a production rate of 300 g/h. The open symbols are 500-3000 particle counts of TEM for each point while filled symbols are nitrogen adsorption data at the filter. Additionally, the evolution of d_S by the proposed model is shown assuming instant droplet evaporation either at x = 0 (solid line) or at x = 7.5 cm (broken lines) corresponding to 2.5 cm below the lowest sampling point [6].

The average primary particle diameters are comparable at x = 20 cm (d_s = 13.6 nm) and the filter location (d_s = 15.3 nm) for the 100 g/h spray and even equal at x = 40 cm (d_s = 26.7 nm) and the filter location (d_s = 26.7 nm) for the 300 g/h spray, indicating that the primary particle growth stops shortly after the particles leave the luminous part of the flame, giving way to the formation of agglomerates, as observed by TEM (Fig. 1). The primary particles made at 100 g/h (d_s = 15.3 nm) are smaller by about 60 % than the ones made at 300 g/h (d_s = 26.7 nm). This is consistent with a $(300/100)^{2/5}$ dependence on the mass or volume aerosol concentration of coagulation-coalescence dominated growth in the free molecular regime [20].

4.2. Particle dynamics and comparison with experimental data

Figure 2 shows the evolution of the d_s as predicted by the proposed model using as initial condition x = 0 cm for a ZrO_2 sintering time based on the approach of Coblenz et al. [21] and for ZrO_2 sintering diffusion coefficient given by Madeyski and Smeltzer [22], along with the experimental measurements for a ZrO_2 powder production rate of 100 g/h (triangles) and 300 g/h (circles). Assuming complete evaporation and conversion to ZrO_2 of the precursor at x = 0 or 5 and 7.5 cm (2.5 cm below the lowest sampling points of the 100 and 300 g/h spray flame, respectively) affects the evolution of the Sauter mean primary particle diameter only at x < 10 and 20 cm (for the 100 and 300 g/h spray flame respectively), while later on in the spray flame the primary particle diameter becomes quite similar (within 1 nm) independent of the starting locations.

The model predictions show the growth of the d_s in the region (x < 30 cm) of high temperatures where sintering is enhanced and leads to an increase of the primary particle diameter until an asymptotic value is attained, above which primary particle growth stops (Fig. 2). The TEMs (Fig. 1) imply that even further downstream agglomerates are formed, in accordance with the sharp increase of the average number of primary particles per agglomerate, n_p. The evolution of the primary particle diameter and that of the powder collected on the filter is predicted reasonably well by the proposed model (Fig. 2) given its assumptions (neglecting droplet evaporation, precursor release, monodisperse primary and agglomerate particles, etc.).

These results indicate that the present simple model can be used to guide reactor design and operation through the prediction of the degree of agglomeration and the agglomerate collision diameter for the product powder. The model describes well the coagulation-controlled part of the spray flame but has to be extended to study the early formation and growth of the particles.

5. CONCLUSIONS

The evolution of ZrO_2 particle growth in spray flames was investigated experimentally by *in-situ* thermophoretic sampling (TS) and counting 500-3000 particles by TEM image analysis in combination with Fourier transform infrared (FTIR) spectroscopy and theoretically by aerosol coagulation and sintering neglecting precursor evaporation, conversion and particle polydispersity. Increasing the ZrO_2 powder production rate from 100 to 300 g/h increased the product primary particle diameter from 12 to 26 nm, in agreement to model predictions indicating that primary particle growth is dominated by coalescence. The geometric standard deviation of the primary particles, σ_{gp}, decreased continuously with increasing height above nozzle for both production rates, indicating that the difference in particle residence time histories from droplet evaporation and precursor release had resulted in broad particle size distributions early on in the flame. Further downstream, coagulation and sintering reduced the σ_{gp} continuously while the collected particle size distribution on the filter was broadened slightly again arising from mixing of particles formed at different streamlines. The simple model predicted well the evolution of particle diameter also indicating that coagulation and sintering may determine solid particle formation in liquid-fed as well as vapor-fed flame aerosol reactors.

6. REFERENCES

[1] L. Mädler, H. K. Kammler, R. Mueller, and S. E. Pratsinis, "Controlled synthesis of nanostructured particles by flame spray pyrolysis," *Journal of Aerosol Science*, vol. 33, pp. 369-389, 2002.

[2] R. Mueller, L. Mädler, and S. E. Pratsinis, "Nanoparticle synthesis at high production rates by flame spray pyrolysis," *Chemical Engineering Science*, vol. 58, pp. 1969-1976, 2003.

[3] T. Tani, K. Takatori, N. Watanabe, and N. Kamiya, "Metal oxide powder synthesis by the "emulsion combustion" method," *Journal of Materials Research*, vol. 13, pp. 1099-1102, 1998.

[4] T. Tani, N. Watanabe, K. Takatori, and S. E. Pratsinis, "Morphology of oxide particles made by the emulsion combustion method," *Journal of the American Ceramic Society*, vol. 86, pp. 898-904, 2003.

[5] L. Mädler and S. E. Pratsinis, "Bismuth oxide nanoparticles by flame spray pyrolysis," *Journal of the American Ceramic Society*, vol. 85, pp. 1713-1718, 2002.

[6] R. Mueller, R. Jossen, H. K. Kammler, S. E. Pratsinis, and M. K. Akhtar, "Growth of zirconia particles made by flame spray pyrolysis," *AIChE J.*, pp. in press, 2004.

[7] M. J. Mayo, J. R. Seidensticker, D. C. Hague, and A. H. Carim, "Surface chemistry effects on the processing and superplastic properties of nanocrystalline oxide ceramics," *Nanostructured Materials*, vol. 11, pp. 271-282, 1999.

[8] T. Chraska, A. H. King, and C. C. Berndt, "On the size-dependent phase transformation in nanoparticulate zirconia," *Materials Science and Engineering a-Structural Materials Properties Microstructure and Processing*, vol. 286, pp. 169-178, 2000.

[9] M. Gell, "Application opportunities for nanostructured materials and coatings," *Materials Science and Engineering A-Structural Materials Properties Microstructure and Processing*, vol. 204, pp. 246-251, 1995.

[10] H. Gleiter, "Materials with ultrafine microstructures: retrospectives and perspectives," *Nanostructured Materials*, vol. 1, pp. 1-19, 1992.

[11] R. A. Dobbins and C. M. Megaridis, "Morphology of flame-generated soot as determined by thermophoretic sampling," *Langmuir*, vol. 3, pp. 254-259, 1987.

[12] F. E. Kruis, K. A. Kusters, S. E. Pratsinis, and B. Scarlett, "A simple model for the evolution of the characteristics of aggregate particles undergoing coagulation and sintering," *Aerosol Science and Technology*, vol. 19, pp. 514-526, 1993.

[13] J. H. Seinfeld, *Atmospheric Chemistry and Physics of Air Pollution*. New York: John Wiley and Sons, 1986.

[14] W. Koch and S. K. Friedlander, "The Effect of Particle Coalescence on the Surface-Area of a Coagulating Aerosol," *Journal of Aerosol Science*, vol. 20, pp. 891-894, 1989.

[15] A. Bejan, *Convection Heat Transfer*. New York: John Wiley and Sons, 1984.

[16] G. D. Byrne, "Pragmatic experiments with Krylov methods in the stiff ODE setting," in *Computational Ordinary Differential Equations*, I. Gladwell, Ed. Oxford: Oxford Univ. Press, 1992, pp. 323-356.

[17] P. T. Spicer, O. Chaoul, S. Tsantilis, and S. E. Pratsinis, "Titania formation by $TiCl_4$ gas phase oxidation, surface growth and coagulation," *Journal of Aerosol Science*, vol. 33, pp. 17-34, 2002.

[18] S. E. Pratsinis, O. Arabi-Katbi, C. M. Megaridis, P. W. Morrison Jr., S. Tsantilis, and H. K. Kammler, "Flame synthesis of spherical nanoparticles," in *Metastable, Mechanically Alloyed and Nanocrystalline Materials, Pts 1 and 2*, vol. 343-3, *Materials Science Forum*. Zurich-Uetikon: Trans Tech Publications Ltd, 2000, pp. 511-518.

[19] S. E. Pratsinis, "Flame aerosol synthesis of ceramic powders," *Progress in Energy and Combustion Science*, vol. 24, pp. 197-219, 1998.

[20] W. Koch and S. K. Friedlander, "Particle growth by coalescence and agglomeration," *Particle & Particle Systems Characterization*, vol. 8, pp. 86-89, 1991.

[21] W. S. Coblenz, J. M. Dynys, R. M. Cannon, and R. L. Coble, "Initial stage solid state sintering models. A critical analysis and assessment," in *Sintering Processes, Material Science Research*, vol. 13, G. C. Kuczynski, Ed. New York: Plenum, 1980, pp. 141-157.

[22] A. Madeyski and W. W. Smeltzer, "Oxygen diffusion in monoclinic zirconia," *Materials Research Bulletin*, vol. 3, pp. 369-376, 1968.